

Pore-scale processes that control dispersion of colloids in saturated porous media

Maria Auset and Arturo A. Keller

Bren School of Environmental Science and Management, University of California, Santa Barbara, California, USA

Received 24 October 2003; revised 8 January 2004; accepted 14 January 2004; published 5 March 2004.

[1] Colloidal dispersion in porous media is a consequence of the different paths and velocities experienced by the colloids. We examined at the pore scale the effect of particle and pore size on colloid dispersion using water-saturated micromodels. The micromodels were produced with polydimethylsiloxane (PDMS), using a soft photolithography technique that allows creating transparent patterns that have dimensions in the range of those existing at the pore space. Four sizes of colloids were transported at several total pressure differences, and image analysis was used to determine particle trajectories, residence times, and dispersion coefficients through the micromodels. The magnitude of the dispersion at any given flow rate was found to be controlled by the pore-space geometry and the relative size of colloids with regards to pore channels. Dispersion coefficient and dispersivity decrease with increasing colloid size. Dispersivity is thus not just a function of pore geometry but depends on colloid characteristics. Because of their size, larger colloids travel in the center streamlines, leading to faster velocities, less detours, and thus lower range of transit times. These findings emphasize the role of particle and pore size on colloidal dispersion and have significant implications for predicting the movement of colloids through saturated porous media. *INDEX TERMS:* 1832 Hydrology: Groundwater transport; 1829 Hydrology: Groundwater hydrology; 1831 Hydrology: Groundwater quality; *KEYWORDS:* Porous media, colloid, dispersion, saturated conditions, pore-scale, geometry

Citation: Auset, M., and A. A. Keller (2004), Pore-scale processes that control dispersion of colloids in saturated porous media, *Water Resour. Res.*, 40, W03503, doi:10.1029/2003WR002800.

1. Introduction

[2] Understanding the factors governing the migration of colloids in the subsurface is important in order to preserve water supply resources and it has been the focus of increased scientific investigation. There are several classes of colloids, biotic and abiotic. Among biotic colloids, significant attention has been given to viruses [Burge and Enkiri, 1978; Pieper et al., 1997; Bales et al., 1997; Woessner et al., 2001], bacteria [Edniond, 1976; Harvey et al., 1989] and protozoa [Sinclair and Ghiorse, 1987; Harvey et al., 1995; Harter et al., 2000]. The motivation comes from a growing concern about potential health problems from contaminated drinking water aquifers [Hejkal et al., 1982] and bioremediation strategies that introduce exogenous bacteria strains [Straube et al., 2003]. In addition mobile colloidal particles may also facilitate the transport of strongly sorbing contaminants like radionuclides [Degueldre, 1997], heavy metals [Corapcioglu and Jiang, 1993] and organic contaminants [Backhus and Gschwend, 1990].

[3] Considerable advances have been made on the prediction of colloidal transport using experimental laboratory and field studies as well as numerical models [McDowell-Boyer et al., 1986; Hornberger et al., 1992; Johnson et al., 1996; McGechan et al., 2002]. However certain mechanisms remain unclear. Early breakthrough of colloids rela-

tive to conservative dissolved tracers has been observed but the processes that control it are not well defined. Colloid dispersion can in part be explained by pore size exclusion [Sirivithayapakorn and Keller, 2003; Bales et al., 1989; Dong et al., 2002; Harter et al., 2000]. Exclusion refers to the fact that although soluble tracers are sufficiently small (on the order of nanometers or less) to move into many or all of the pore spaces in the porous media, colloids, due to their physical size (on the order of hundreds to thousands of nanometers), may not enter small pores. Sirivithayapakorn and Keller [2003] determined a pore throat to colloid diameter threshold of about 1.5 for entering a pore, which means that colloids larger than about 1–2 μm are excluded from most small pore throats. Larger colloids will thus travel through a reduced number of pathways, which on average decreases their travel time.

[4] Similarly, colloids can be excluded from lower-velocity streamlines near pore walls. This process results in another increase in average velocity of colloids with respect to conservative tracers. DiMarzio and Guttman [1970] proposed this concept to explain their theory of particles separation by flow. Small [1974] proposed the “hydrodynamic chromatography” technique for the size analysis of colloidal particles. Avogadro and de Marsily [1984] suggested that colloid migration in porous media might be similar to that occurring in hydrodynamic chromatography.

[5] Theoretical models in the literature represent the effects of particle exclusion from certain pore throats or

streamlines near the pore wall by the application of an acceleration factor or the reduction of the effective porosity available to the colloids [Morley *et al.*, 1998; Harter *et al.*, 2000]. This approach has been questioned by several authors [e.g., Mailloux *et al.*, 1999; Scheibe and Wood, 2003] mainly because it leads to an increase in dispersion, inconsistent with a phenomenon that reduces the velocity variance and limits access to some regions. Instead, Scheibe and Wood [2003] propose to model the exclusion phenomena by truncating the distribution of local dispersive displacements at the lower end.

[6] To account for colloid exclusion processes and the corresponding velocity increase or “acceleration,” other authors have chosen to represent the porous medium as a series of straight parallel tubes of constant cross-section [e.g., Nagasaki *et al.*, 1993]. This approach ignores the details of the morphology of the pore space, i.e., its obstacles and intersections at pore bodies, which has a significant effect on the streamlines and hence modifies dispersion. Grindrod *et al.* [1996] already point out that earlier colloid breakthrough does not necessarily imply a higher mean elution rate but rather a lower effective dispersion rate. James and Chrysikopoulos [2003] show mathematically that size exclusion of particles flowing in a saturated fracture increases the particle effective velocity and decreases its effective dispersion coefficient. Sirivithayapakorn and Keller [2003] found that in a complex pore space, colloids of different diameters will travel through different pathways, with a corresponding effect on both mean velocity and dispersion.

[7] Conventional modeling of transport processes is based on the macroscopic advective-dispersive equation (ADE):

$$\frac{\partial C}{\partial t} = \nabla \cdot (\mathbf{D} \cdot \nabla C) - \nabla \cdot (\mathbf{v}C) \quad (1)$$

where t is time, C is concentration, \mathbf{D} is the dispersion coefficient tensor, and \mathbf{v} is the velocity vector.

[8] Hydrodynamic dispersion characterizes the spreading of substances in porous media during water flow. Under saturated conditions the dispersion coefficient is expressed as [Bear, 1988]:

$$D_L = D_0 + \alpha v^n \quad (2)$$

where D_0 is the effective molecular diffusion in the porous media ($L^2 T^{-1}$); α is the dispersivity (L), and n is an experimental constant. In the case of nonaggregated sands or glass beads and at high Peclet number, n can be considered equal to unity [Bolt, 1979]. Dispersivity is assumed to be an intrinsic medium property [Fried and Combarnous, 1971] and is a required input parameter in transport models based on the ADE [Zheng and Bennett, 1995].

[9] The aim of this research is to study colloid exclusion on the basis of dispersion of colloids of different sizes using some distinct pore geometries that serve to better distinguish between processes and their relative importance. We seek to understand the relationship between colloid size, exclusion processes and dispersion. Our experiments are conducted at the pore-scale using micromodels under water-saturated conditions. The results provide a mechanistic insight into

the nature of the exclusion processes at the pore scale, and their effect on dispersion and dispersivity.

2. Materials and Methods

2.1. Micromodels

[10] The micromodels were fabricated using a silicone elastomer poly(dimethylsiloxane) (PDMS) by a soft photolithography technique according to the experimental procedure developed by Quake and Scherer [2000].

2.1.1. Micromodel Fabrication

[11] The network of micromodel channels (with width ≥ 5 microns) was designed with a Computer Aided Design program (L-edit) commonly used to design integrated circuits. A high-resolution printer converted this design into a transparency, printing the pattern and leaving the background clear; this transparency was used as a mask on a silicon wafer. The wafer was spin-coated with positive photoresist to create a master, using photolithography.

[12] To mold each micromodel a 5:1 mixture of PDMS prepolymer and curing agent (R.S. Hughes, Silicone Rubber RTV 615) was stirred thoroughly. The polymer mixture was then poured in a Petri dish containing the patterned silicon wafer. After pouring, the polymer was degassed under vacuum for approximately 1 hour until air bubbles no longer rose to the top and then was cured for 15 minutes at 65°C. After curing, the polymer was peeled from the mold and holes providing access to the channels were punched through the bulk material with a 1 mm diameter blunt needle (Intramedic 427565 gauge 23). The device was then placed on a precured thin slab of PDMS (4:0.2 mixture of PDMS prepolymer and curing agent) in order to form a closed channel system of four equivalent walls and polymerized for 12 h at 60°C.

2.1.2. Characteristics of the Micromodels

[13] The PDMS micromodel surface is intrinsically hydrophobic with a contact angle close to 109° [Hu *et al.*, 2002]. The pattern used for each micromodel had a quadrilateral network of 100 large pore spaces (pore bodies) approximately 60 μm in diameter connected by mutually perpendicular narrow channels (or pore throats). Dullien and Dhawan [1974] suggested that the void space in natural porous media is an arrangement of converging and diverging channels with a distribution of sizes. Three micromodel patterns were designed, differing in channel layout (Figure 1): (1) micromodel A, a narrow regular network with constant channel width of 10 μm , (2) micromodel B, a wide regular network with constant channel width of 20 μm , and (3) micromodel C, a zigzag network with two different channel widths, 10 and 20 μm . We controlled the etching process to produce an almost constant depth of 12 μm . A scanning electron micrograph (SEM) of the pore space is presented in Figure 2.

[14] The physical and hydraulic properties of the micromodels are shown in Table 1. Porosities were calculated using the ratio of measured pore void area to total area. The areas were estimated from the L-edit design. We employed the Kozeny-Carman equation [Bear, 1988] to estimate the micromodel's permeability:

$$k = \frac{d_m^2}{180} \frac{\theta^3}{(1 - \theta)^2} \quad (3)$$

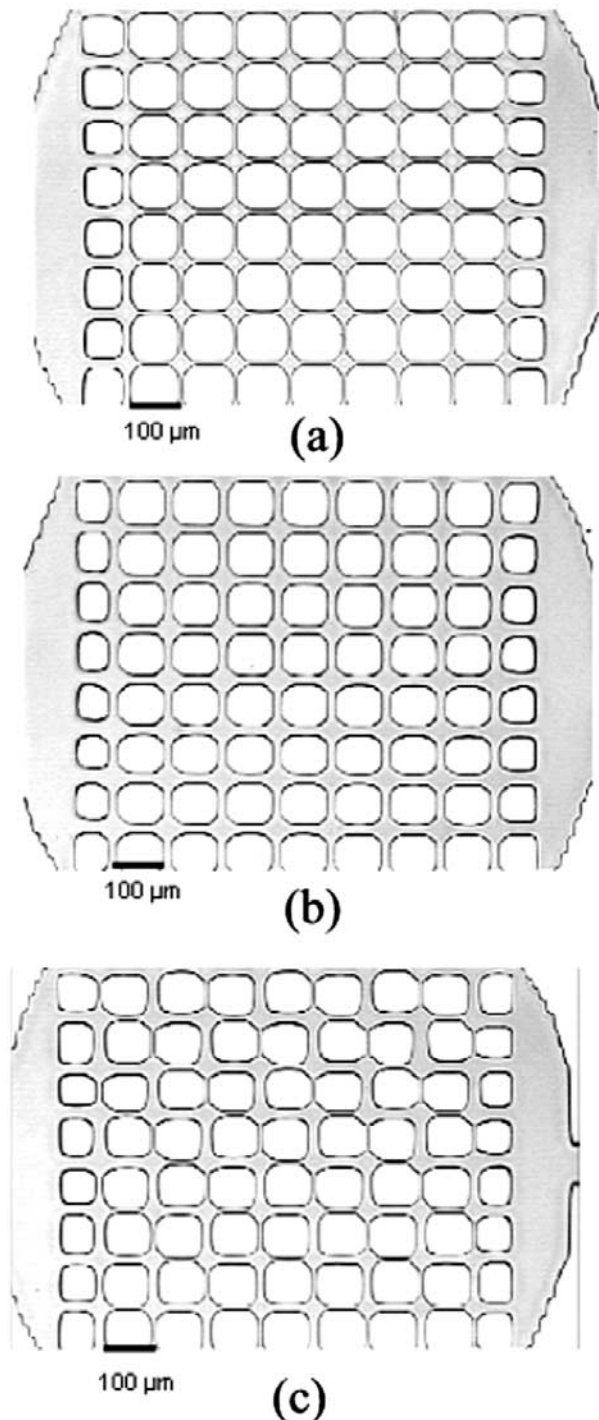


Figure 1. Optic microscope images of the polymer replica obtained from the silicon wafer, containing a pattern of channels for (a) micromodel A, (b) micromodel B, and (c) micromodel C. The inlet and outlet ports are placed on each side of the network from left to right or right to left in this image. The scale bar gives an indication of the width of the pore space.

where d_m is mean size of the solid matrix that creates pores and channels and θ is the porosity of each micromodel.

2.2. Colloidal Particles

[15] The colloids employed consisted of carboxylate-modified latex polystyrene microspheres with a very narrow

size distribution (Duke Scientific Corporation, Palo Alto, California) labeled with a green fluorescent dye (Excitation/Emission = 468/508 nm). Four different sizes of microspheres (2, 3, 5, and 7 μm in diameter) were used. These microspheres have been employed in previous studies reported in the literature [e.g., Palmer *et al.*, 1999; Huettel and Rusch, 2000]. Given that our work focuses only on transport of colloids such as microorganisms in the absence of attachment and growth, microspheres with precise diameters and known surface chemistry can be used as surrogates. The microbeads employed were negatively charged because of the carboxyl groups grafted on their surface. They were slightly hydrophobic, had a density of 1.05 g/cm^3 and a refractive index of 1.59 at 589 nm (according to manufacturer data sheet).

[16] The colloids were suspended in a solution buffered at pH 7.8 to minimize colloid adhesion to each other. Microsphere concentrations in the suspensions were determined by filtration through 25 mm membrane filters (Whatman) and counting with epifluorescent microscopy. The range of the colloid concentrations used in our experiments was 10^6 – 10^7 colloids per mL.

2.3. Experimental Setup and Procedures

[17] To inject the colloidal suspension, a 10 mL glass syringe (number 1010, Hamilton Co., Reno, Nevada) was used, with 1 mm external diameter polyethylene tubing (Intramedic 427410) and an adapter (Intramedic 427565 gauge 23) connecting the syringe to the horizontally mounted micromodel. The micromodel was placed underneath the objective of an epifluorescent microscope (Nikon Optiphot-M) equipped with a Charged-Coupled Device (CCD) camera (Optronics Engineering) capturing at a frequency of 60 frames/s. The signal from the camera was fed to a Sony Trinitron monitor that allowed displaying real-time movement of the colloids and to a digital camera (Sony Digital Handycam) for monitoring and recording the experiments.

[18] The study was conducted under water-saturated conditions and under four total pressure differences: 100, 500, 1000 and 1500 Pa. Total pressure difference was induced by gravity and controlled by the height of the open glass syringe relative to the micromodel. Flow rate was measured at the inlet, using a digital flowmeter (Fischer Scientific Model 1000).

[19] Distilled water was used to fully saturate the micromodel before an experiment began. At least 10 pore volumes of distilled water were flushed through the model to remove any air bubbles. After steady state flow was established, each colloidal suspension was injected into the saturated micromodel. Monodisperse suspensions of homogeneous colloid size were injected separately, to monitor their transport behavior independently. The movement of the colloids was observed at 5X and 10X magnification and recorded in real time on the digital camera.

[20] Since the focus of this study was colloidal migration and dispersion processes, we did not focus on either filtration or attachment mechanisms. Thus we exclude reporting here on experiments in which colloids became attached in pore throats. These trapped colloids by their mere presence reduce pore space to the flowing colloids and consequently alter the streamlines and pressure field. Actually a number of our experiments had to be repeated due to

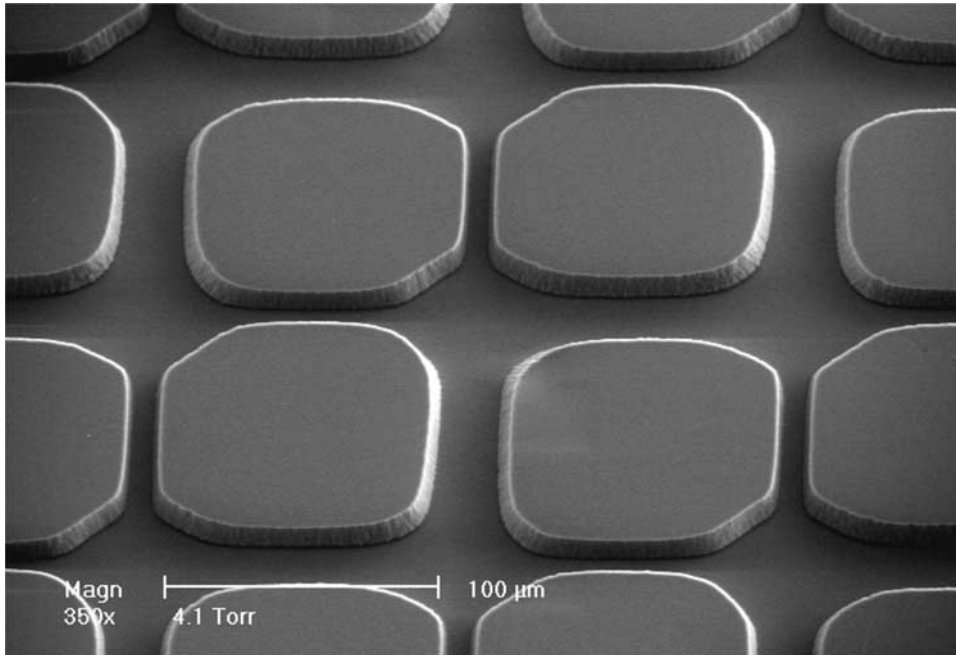


Figure 2. Scanning electron micrograph of the pore space in the zigzag network micromodel with 10 and 20 μm channel widths.

pore clogging. We are investigating colloid attachment in separate studies.

2.3.1. Image Analysis Technique

[21] The migration of the particles was captured by video microscopy. Video image analysis was then performed using IDL[®] software (Interactive Data Language) which is a programming language commercialized by Research Systems, Inc (RSI). Particle trajectories were determined for at least 1000 colloids and pathway lengths and residence times were extracted by processing at least 100 different individual colloids for each pressure, micromodel and colloid size.

[22] Femlab (COMSOL, Inc.), a finite element code developed for the Matlab environment, was used to calculate the flow streamlines within the micromodels, to explain the behavior based on fluid dynamics point of view.

2.3.2. Dispersion Calculation

[23] From the trajectory data, the number and frequency of detours taken by the colloids along the path were determined. A full detour was defined as a 90° turn made by a colloid into a channel perpendicular to the main flow direction followed by a second 90° turn into a different channel parallel to the main flow direction.

[24] We estimated the value of the longitudinal dispersion coefficient D_L using the relationship [Fetter, 1999]:

$$D_L = \frac{\sigma_L^2}{2t} \quad (4)$$

where t is the time and σ_L^2 is the spatial variance in the direction of flow, which is calculated from individual trajectories using:

$$D_L = \frac{1}{N} \sum_i \frac{(d_i - \bar{L})^2}{2t_i} \quad (5)$$

where \bar{L} is the average pathway length of the whole group of particles inside the micromodel from the inlet to the

outlet, d_i is the trajectory length of an individual particle, i , and t_i is the residence time of an individual particle through the porous space. The standard deviation was derived numerically from the pathway distance distribution. The calculation of each dispersion coefficient involves at least 100 particles.

3. Results and Discussion

3.1. Trajectories

[25] The trajectories of four different sizes of colloids were analyzed within three different geometries. The observed preferential paths in the regular micromodels (models A and B) were the straight trajectories, that is, the most direct and shortest route through pore throats aligned with the pressure gradient. However, in some cases, the colloids would take one or two detours. The path lines of ten $3 \mu\text{m}$ particles in model B are depicted in Figure 3 as an example for the regular $20 \mu\text{m}$ network. The first seven trajectories from the top are straight without detours; the three others include one or two detours. The trajectories depicted here are not representative of the frequency of detours but rather serve to illustrate the concepts.

[26] Because of the more tortuous geometry, colloids took more detours in the zigzag pore space (Figure 4). All

Table 1. Physical and Hydraulic Properties of Micromodels

	Micromodel		
	A	B	C
Length, mm	1	1	1
Width, mm	0.8	0.8	0.8
Porosity	0.228	0.358	0.278
Thickness, mm	1.2×10^{-2}	1.2×10^{-2}	1.2×10^{-2}
Pore volume, mm^3	2.7×10^{-3}	4.3×10^{-3}	3.3×10^{-3}
Permeability, mm^2	1.2×10^{-6}	6.2×10^{-6}	2.6×10^{-6}

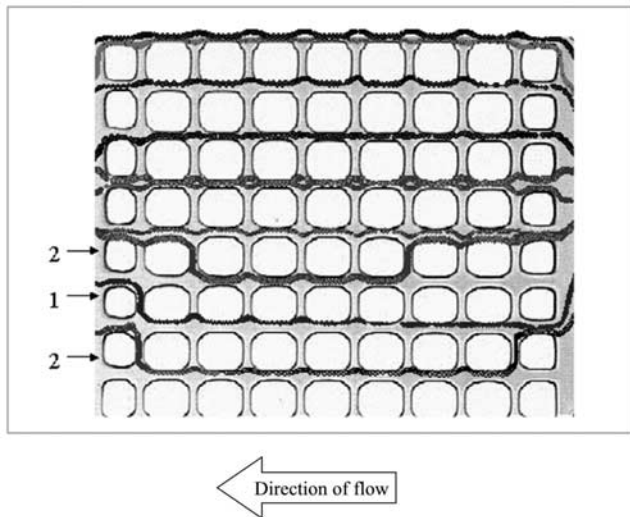


Figure 3. Several randomly chosen trajectories of ten 3 μm particles in the regular 20 μm network. The seven first trajectories from the top are straight (any detour); the three last trajectories make one or two detours. Numbers at the left indicate the numbers of detours.

detours were initiated as particles traveling in a wide channel approach a narrow channel in the general flow direction. Although a small fraction proceeds into the narrow channel, there is a high probability that they will detour into the perpendicular channels. More than 70% of the detours were made into a wide channel. It must be noted that all detours into narrow channels were made after a detour into a wide channel.

[27] The frequency and number of colloidal detours are compared in Figure 5 for the four particle diameters, three micromodels and four total pressure differences. These results represent the statistics of over 1000 particles per experiment. The left column corresponds to the regular network with 10 μm pore throats, the second column represents the regular 20 μm network and the right column presents data from the zigzag pattern. We can see that, in general, the number of detours increased with increasing total pressure difference (increasing from top to bottom in Figure 5). In the regular micromodels and under the same pressure, as the particle size to pore channel width ratio increases, the number of detours through the micromodel decreases. The 5 μm and 7 μm particles flowed all the way through the narrowest pore space without detours for at least 1000 particles. However, as particle diameter decreased the frequency of detours increased; consequently the particles followed a more tortuous path within the pore space augmenting their hydrodynamic dispersion.

[28] In the zigzag pattern, odd-numbered sets of detours were most frequent. Note that 5 and 7 detours were observed in this more complex geometry, and that even the largest colloids were detoured to some extent. As in the regular networks smaller colloids took more detours. *Sirivithayapakorn and Keller* [2003] also observed that smaller particles changed paths more often than larger particles and hence have a more diverse path flow in a more realistic and complex micromodel of porous media.

[29] Figure 6 presents the pathways of 2 μm colloids within the zigzag micromodel performed after analysis with

IDL. Figure 6 shows that particles traveling in the region closest to the channel wall (e.g., orange path) were generally detoured, i.e., they were more likely to move into the perpendicular pore throats because they were moving along the flow streamlines that deviated most when crossing a pore body. On the other hand, colloids traveling near the center of the channel (e.g., light green path) were likely to continue their journey without detours. Note however that the particle (black path) near the “top” of Figure 6 (all are in a horizontal plane) must have moved via Brownian motion to a different streamline, which resulted in only one detour after having traveled mostly in the centerline.

[30] Figure 7 presents the flow pathways calculated by solving the Navier-Stokes equations at the pore scale using FEMLAB. Note that the streamlines near the channel walls lead into the 90° detours, and that the effect is much stronger in the zigzag geometry. The streamlines fan out and converge in each pore body, but this process leads to some streamlines that deviate into a detour. *Sahimi et al.* [1986] also calculated numerically a similar streamline distribution for a regular square network. The streamline distribution helps to explain the relationship between number of detours and colloid size. A particle transfers randomly via Brownian motion over the different flow streamlines between the walls of the channel, while being carried downstream by flow. However when particle size is a significant fraction of channel width, the particle is constrained to the central streamlines, with a reduced likelihood of detours and thus establishing preferential straight trajectories.

[31] It becomes clear that a parallel capillary tube analogy is incorrect, since it does not allow for particle detours; dispersion of these colloids is not just related to the velocity profile in a channel, but also has to take into account the complex pathways taken by some particles through the pore network.

[32] In all cases we observed, when a particle undergoes multiple detours in the regular pattern, the particle returns to the initial channel, as shown in Figure 6. This observation is consistent with the Navier-Stokes simulation results

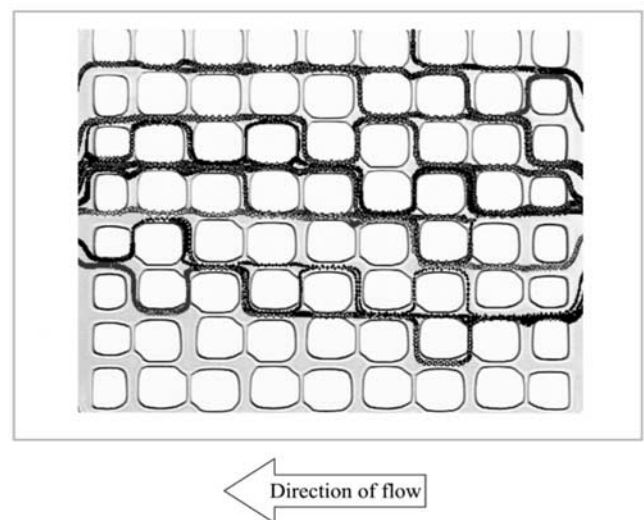


Figure 4. Several randomly chosen trajectories of 3 μm colloids in the zigzag network.

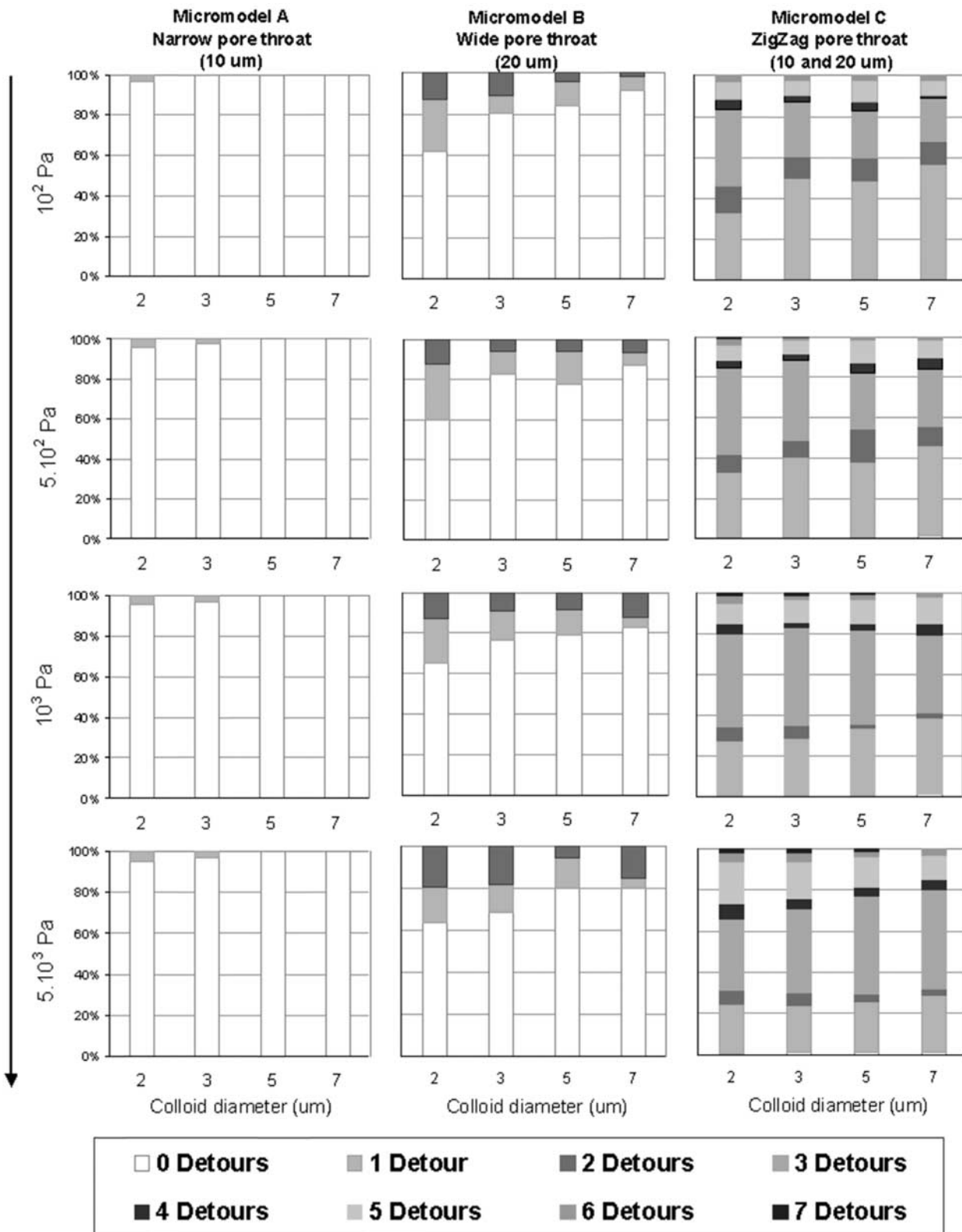


Figure 5. Frequency and number of detours in the regular narrow micromodel (first column), in the regular wide (second column), and in the zigzag micromodel for four colloid sizes and four pressures (third column). See color version of this figure at back of this issue.

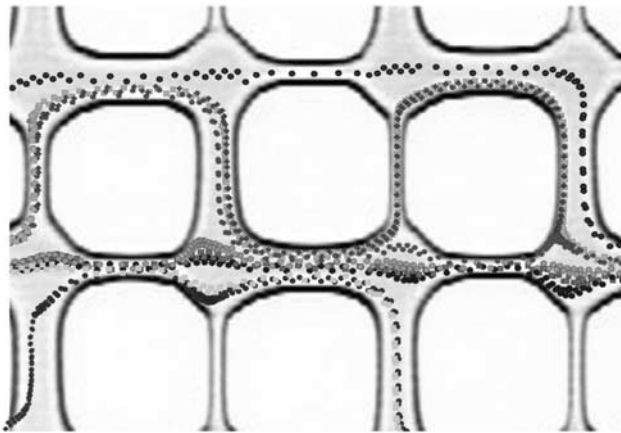


Figure 6. Detail of 2 μm colloid trajectories in the zigzag micromodel analyzed using IDL[®]. The colors indicate different particles tracked at different times but superimposed here to illustrate the different pathways. See color version of this figure at back of this issue.

(Figure 7), which show how the streamlines near the walls meander among channels but are naturally always close to the wall. This reflects the fact that these particles are essentially remaining in the streamlines near the walls, and do not undergo significant diffusion within the channel, even as they go through multiple detours. Note that the observation path length is small (1 mm); this effect is likely to vary across larger scales, as there is more time for random movements to disperse the particles.

[33] As the total pressure difference across the zigzag micromodel increases, the number of detours through the widest channels increases, as shown in Figure 8, with more noticeable effect for the 7 μm colloids. Thus colloids preferentially enter larger pore throats, suggesting a size exclusion effect, based on the ratio of colloid to pore throat dimensions.

[34] Detours have a significant effect on particle residence time within the different micromodels, since the flow velocity in the channels perpendicular to the pressure gradient is much lower. Since smaller particles are more likely to sample a range of streamlines, including those near the walls, they are more likely to detour into slow channels and thus exhibit a wider residence time distribution. As observed by *Sirivithayapakorn and Keller* [2003], the larger colloids travel through a reduced number of pathways, which has an important effect on their arrival time. The observed residence time distribution in the zigzag pore space for 2 μm (Figure 9a) and 7 μm (Figure 9b) colloids at the lower pressure indicates a higher dispersion of the smaller particles.

3.2. Dispersion Coefficient

[35] Figure 10 presents dispersion coefficients plotted against mean velocity for each micromodel and colloid size. The dispersion coefficients obtained from all the experiments increase as a linear function of pore velocity, following equation (2) setting n equal to 1 and neglecting the diffusion term since it is quite small [*Bolt*, 1979; *Sirivithayapakorn and Keller*, 2003]. The highest dispersion coefficient values are found in the zigzag network and the

lowest values in the narrower regular micromodel, which is in good accordance with the number of detours observed in each micromodel (Figure 5). A detoured particle experiences longer residence time because of the longer pathway, the low overall velocity in the channels perpendicular to the pressure gradient, and because a particle that detours is already generally traveling along the streamlines closest to the wall, which are the slowest ones.

[36] The relatively low values of the dispersion coefficients observed in our experiments may be due to the small length scale and the homogeneity of the constructed micromodel networks. For example, in a 4 cm square capillary network, *Lanning and Ford* [2002] calculated a dispersion coefficient of $6 \times 10^{-3} \text{ cm}^2 \text{ s}^{-1}$ when the interstitial

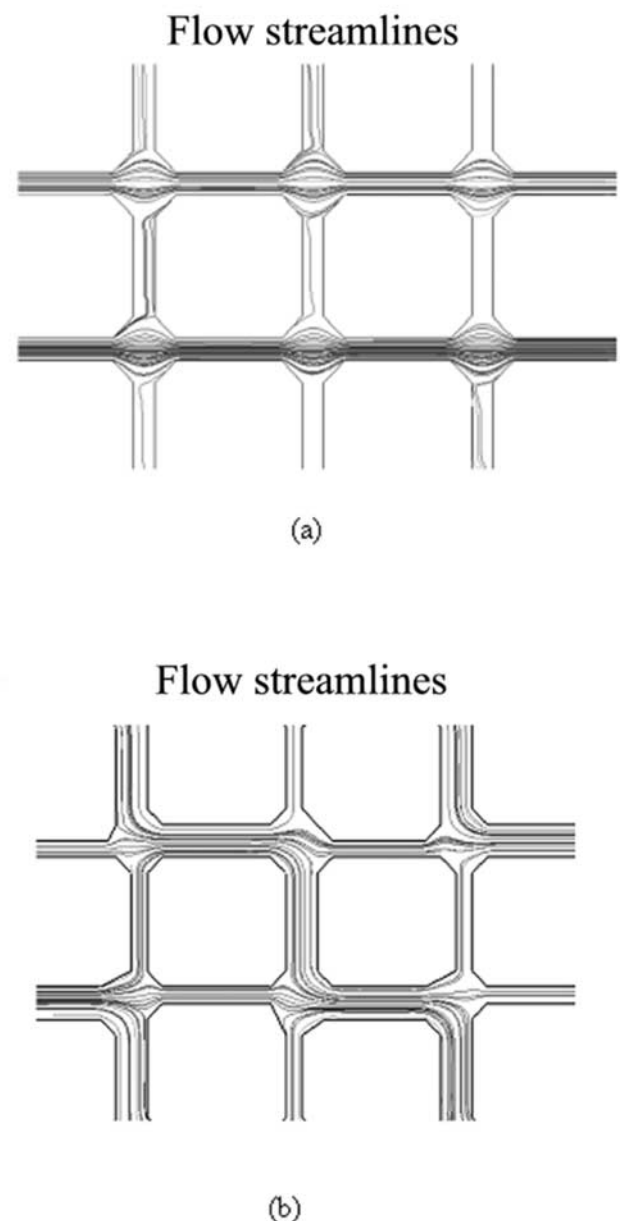


Figure 7. Flow streamlines for (a) regular and (b) zigzag micromodels, calculated using FEMLAB[®].

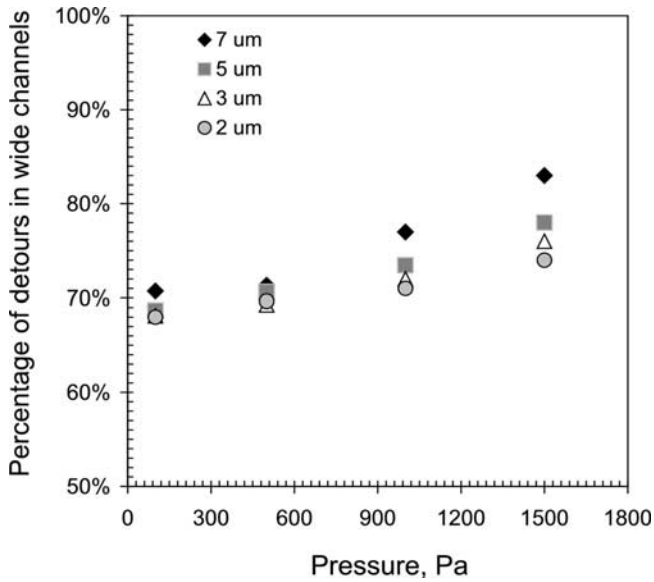
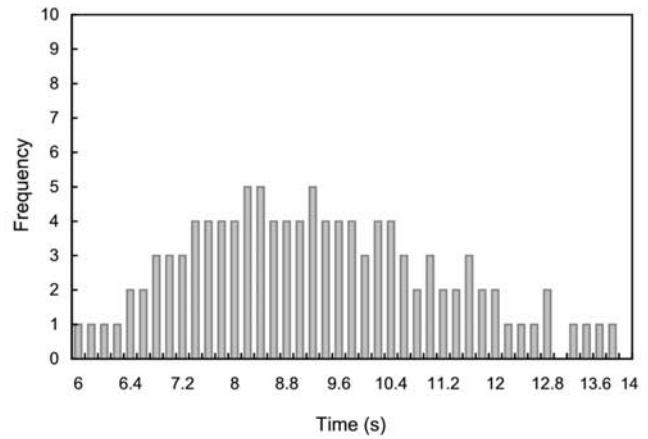


Figure 8. Frequency of detours through wide (20 μm) channels in zigzag micromodel as a function of total pressure difference and colloid diameter. The Y axis scale is from 50 to 100%.

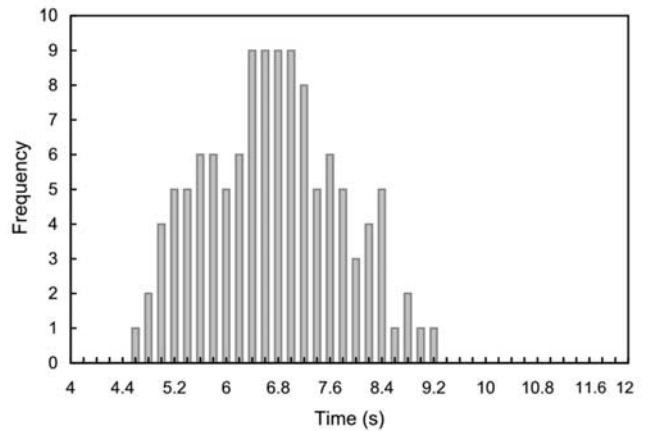
velocity was $3 \times 10^{-2} \text{ cm s}^{-1}$. For the same velocity range we studied, 3 μm colloids traveling in water-saturated sand columns 60 cm in length had a dispersion coefficient value of $2 \times 10^{-4} \text{ cm}^2 \text{ s}^{-1}$ (A. Keller et al., Early breakthrough of colloids and bacteriophage MS2 in a water saturated sand column, submitted to *Water Resources Research*, 2003) (hereinafter referred to as Keller et al., submitted manuscript, 2003). For lower velocities (around $2 \times 10^{-3} \text{ cm s}^{-1}$), Grindrod et al. [1996] and Zhang et al. [2001] found dispersion coefficients in the range of $2 \times 10^{-2} \text{ cm}^2 \text{ s}^{-1}$ for a 1 nm colloid in a sand aquifer and $1.5 \times 10^{-3} \text{ cm}^2 \text{ s}^{-1}$ for a 0.98 μm microsphere in a gravel aquifer, respectively. Our dispersion coefficients are two to four orders of magnitude lower than most of these similar studies at larger scales, with more complex networks and in some cases larger pore water velocities.

[37] The larger the colloid size, the lower the dispersion coefficient, for the same network and pore velocity. This is a function of size exclusion from some narrow pore throats, focusing of large particles in the central streamlines, and detours through a network. Flow streamlines closest to the pore walls detour the most, and experience the lowest velocities in the parabolic Poiseuille profile. However, because of their size, large particles are physically unable to access such streamlines; this leads to two important differences with regards to smaller colloids or a dissolved molecule: (1) travel in the center streamlines is faster than the average flow velocity; and (2) travel in the center streamlines reduces detouring which results in shorter pathways. Therefore large colloids experience a narrower residence time variation. The net result is a colloidal dispersion reduced by a factor that increases with increasing particle size.

[38] These results are consistent with larger-scale observations and theoretical considerations. Colloid breakthroughs often exhibit sharper fronts and higher peaks at the earliest arrivals times relative to ideal tracers, indicating less residence time variability. Field experimental data from



(a)



(b)

Figure 9. Residence time distribution for (a) 2 μm and (b) 7 μm colloids in the zigzag pore space at the lower pressure. We present the same range in the X axis (8 s) for comparison.

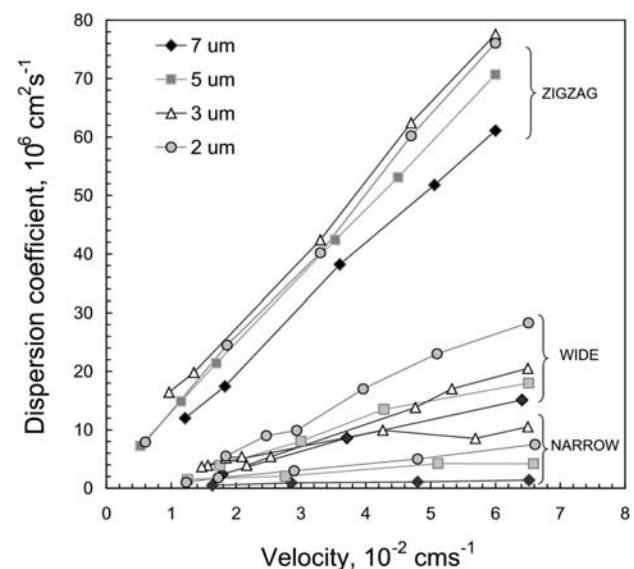


Figure 10. Relationship between dispersion coefficient and velocity for the three micromodels and four colloid sizes.

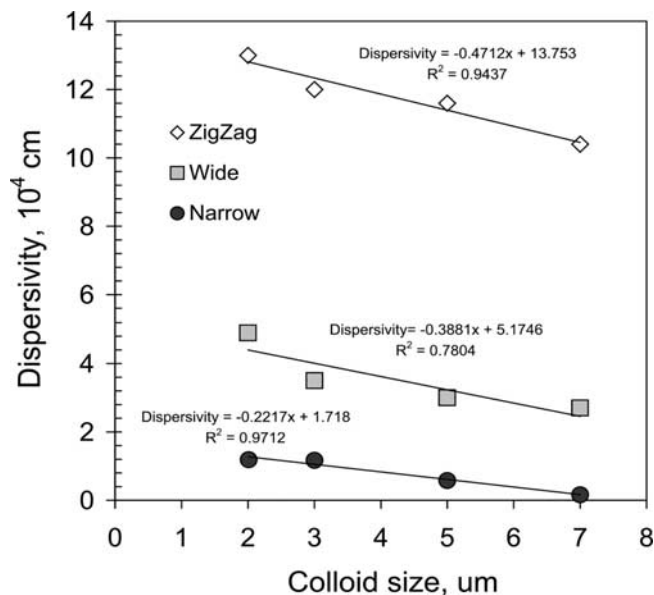


Figure 11. Relationship between dispersivity and colloid size for the three micromodels.

Grindrod *et al.* [1996] indicated that dispersion rates of colloidal particles can be 20% less than for a soluble tracer. Keller *et al.* (submitted manuscript, 2003), showed that dispersion coefficient decreases with colloid size in saturated sand columns. Using a theoretical approach, James and Chrysikopoulos [2003] established that larger particles had smaller effective dispersion within a saturated fracture because of the exclusion of a portion of the velocity profile. Scheibe and Wood [2003] modeled the exclusion phenomena by truncating the lower end of the distribution of longitudinal dispersive displacements. This method leads to decreased apparent dispersion of the colloids relative to soluble tracers. Our findings will serve to establish a better conceptual framework, by providing the mechanisms that result in decreased dispersion based on colloid size.

[39] One important corollary of these results is the finding that dispersivity depends not only on the porous medium's geometry, but also on colloid size. The average longitudinal dispersivity of the micromodels was determined from the slope of the regression line between the dispersion coefficient and the velocity in Figure 10, for each colloid. Figure 11 presents the dispersivity as a function of the colloid size for the three micromodels. For a given network, dispersivity decreases almost linearly with colloid size. Dispersivity is also a function of pore geometry, increasing markedly for the slightly more complex zigzag geometry.

[40] These findings are somewhat unexpected, given that, theoretically, dispersivity is assumed to be an intrinsic soil property and consequently a constant value for a given porous medium [Fried and Combarous, 1971; Bower, 1978]. However, Shonnard *et al.* [1994] and Pang *et al.* [1998], analyzing earlier breakthrough of microbes relative to a tracer, assigned a lower dispersivity for the microbe than for a molecular solute. They stated that differences in dispersion explain the faster breakthrough, although they were unable to pinpoint the mechanism that caused these differences. Sinton *et al.* [2000] reported reductions in the

dispersivity when modeling migration of different sized microorganisms in an alluvial gravel aquifer.

[41] Dispersivity is a required input parameter in colloidal transport models based on the equations (1) and (2). From our results, dispersivity is dependent on colloid size. Therefore dispersivity values estimated from a soluble tracer may not be valid to represent the dispersivity of a colloid. It had previously been noted by Hornberger *et al.* [1992] that bacteria breakthrough observations were inconsistent with dispersivity values estimated from solute transport equations.

[42] From our experimental results, dispersivities for these micromodels range from 1.6×10^{-5} to 1.3×10^{-3} cm. These magnitudes are in the range of values found in literature given that Gelhar [1986] and Russo [2002] documented an increasing dispersivity with the scale of the system. At the pore scale, Lanning and Ford [2002] reported a dispersivity of 0.28 cm and 0.33 cm when a strain of *Escherichia coli* was dispersed in different 4.4 cm long spatially periodic networks. Sinton *et al.* [2000] found dispersivity values that ranged from 0.7 m for *Escherichia coli* to 1.4 m for *Bacillus subtilis* endospores in an aquifer with a screened depth of 18 m.

[43] The analysis presented here concentrated on transport dominated by the nonsorbing colloids that passed freely through the preferential pathways. Under such conditions, advection and hydrodynamic dispersion dominate. However, we observed in our studies that, in the long term, *i.e.*, after injecting about 40 pore volumes, some colloids began to attach to the channel walls. This phenomenon was particularly significant in the case of larger particles and narrower pore throats. Such colloids remained sorbed essentially irreversibly and created large attached clusters that prevented other colloids from passing through. Once a fraction of the pore space was no longer accessible, due to clogging, the remaining channels provided a variety of additional trajectories for the colloids. So as the number of clogged pores increased, the pathways sampled by the colloids became more and more tortuous, leading to the possibility of increased spreading and hydrodynamic dispersion. Although the detoured trajectories caused by clogging were not considered in our analysis, further studies should focus on the influence of colloidal sorption/filtration on dispersion.

[44] From our observations it is to be noted that, in the short term, the size of colloids affects colloidal dispersion through a number of mechanisms. It seems that, in the long term, the finite size of the colloids can also modify the dispersion process by filtration and/or sorption.

4. Conclusion

[45] The polydimethylsiloxane (PDMS) micromodels used in this study allowed direct observation and quantification of colloidal dispersion under water saturated conditions. Colloidal dispersion in a porous media is a consequence of the different paths and velocities experienced by the colloids. Our study focused on the transport of nonsorbing colloids, that is, colloids that did not experience filtration or attachment. Under such conditions, larger particles preferentially experience straighter pathways, whereas smaller particles make more detours. The magnitude of the dispersion at any given flow rate is not only

controlled by the pore-space geometry but also by the size of the pore channels and the size of the colloids. Dispersion coefficients and dispersivity decrease with increasing colloid size. Because of their size, large particles are excluded from the streamlines that detour the most and experience the highest velocity in a parabolic Poiseuille's profile. At the pore scale this effect can result in relatively large differences in dispersion.

[46] These pore-scale results have important implications for understanding and predicting the breakthrough of colloids. First, dispersivity is a function not only on the porous medium, but also of colloid size. Simulations of colloid transport that consider a constant dispersivity may be in significant error. Field tests using traditional tracers might result in an overestimation of the dispersion of different-sized colloids. Even field tests with colloidal tracers need to take into consideration this effect. Second, our results provide a mechanistic explanation of the nature of these differences in dispersivity. Larger colloids are not only excluded from entering smaller pores, they also travel in the center streamlines due to their size, which results in faster travel velocities and less detouring. These findings emphasize the importance of considering the relative size of the particle with regards to pore channels when predicting colloidal dispersion, and provide a better basis for modeling the movement of colloids through saturated porous media.

[47] **Acknowledgments.** The authors gratefully acknowledge David Pine and Eric Michel (Chemical Engineering Department, UCSB) for technical assistance and equipment for micromodel fabrication and in data analysis. M. Auset thanks the postdoctoral fellowship supported by the Secretaría de Estado de Educación y Universidades (Spain) and partially supported by European Social Fund. The authors also wish to acknowledge partial funding from U.S. EPA Exploratory Research grant R826268 and US EPA grant R827133, as well as from the University of California Water Resources Center and the UCSB Academic Senate.

References

- Avogadro, A., and G. de Marsily (1984), The role of colloids in nuclear waste disposal, *Mater. Res. Soc. Symp. Proc.*, 26.
- Backhus, D. A., and P. M. Gschwend (1990), Fluorescent polycyclic aromatic hydrocarbons as probes for studying the impact of colloids on pollutant transport in groundwater, *Environ. Sci. Technol.*, 24, 1214–1223.
- Bales, R. C., C. P. Gerba, G. H. Grondin, and S. L. Jensen (1989), Bacteriophage transport in sandy soil and fractured tuff, *Appl. Environ. Microbiol.*, 55, 2061–2067.
- Bales, R. C., S. M. Li, T. C. J. Yeh, M. E. Lenczewski, and C. P. Gerba (1997), Bacteriophage and microsphere transport in saturated porous media: Forced-gradient experiment at Borden, Ontario, *Water Resour. Res.*, 33, 639–648.
- Bear, J. (1988), *Dynamics of Fluids in Porous Media*, 764 pp., Dover, Mineola, N. Y.
- Bolt, G. H. (1979), Movement of solutes in soil: Principles of adsorption/exchange chromatography, in *Soil Chemistry: B. Physico-chemical Models*, pp. 285–348, Elsevier Sci., New York.
- Bouwer, H. (1978), *Groundwater Hydrology*, McGraw-Hill, New York.
- Burge, W. D., and N. K. Enkiri (1978), Virus adsorption by 5 soils, *J. Environ. Qual.*, 7, 73–76.
- Corapcioglu, M. Y., and S. Y. Jiang (1993), Colloid-facilitated groundwater contaminant transport, *Water Resour. Res.*, 29, 2215–2226.
- Degueldre, C. (1997), Groundwater colloid properties and their potential influence on radionuclide transport, *Mater. Res. Soc. Symp. Proc.*, 465, 835 pp.
- Dimarzio, E. A., and C. M. Guttman (1970), Separation by flow, *Macromolecules*, 3, 131–146.
- Dong, H., T. C. Onstott, M. F. DeFlaun, M. Fuller, T. D. Scheibe, S. H. Streger, R. K. Rothmel, and B. J. Mailloux (2002), Relative dominance of physical versus chemical effects on the transport of adhesion deficient bacteria in intact cores from South Oyster, Virginia, *Environ. Sci. Technol.*, 36, 891–900.
- Dullien, F. A. L., and G. K. Dhawan (1974), Characterization of pore structure by a combination of quantitative photomicrography and mercury porosimetry, *J. Colloid Interface Sci.*, 47, 337–349.
- Edmond, R. L. (1976), Survival of coliform bacteria in sewage sludge applied to a forest clearcut and potential movement into groundwater, *Appl. Environ. Microbiol.*, 32, 537–546.
- Fetter, C. W. (1999), *Contaminant Hydrogeology*, 2nd ed., Prentice-Hall, Old Tappan, N. J.
- Fried, J. J., and M. A. Combarous (1971), Dispersion in porous media, *Adv. Hydrosci.*, 7, 169–282.
- Gelhar, L. W. (1986), Stochastic subsurface hydrology from theory to applications, *Water Resour. Res.*, 22, S135–S145.
- Grindrod, P., M. S. Edwards, J. J. W. Higgs, and G. M. Williams (1996), Analysis of colloid and tracer breakthrough curves, *J. Contam. Hydrol.*, 21, 243–253.
- Harter, T., S. Wagner, and E. R. Atwill (2000), Colloid transport and filtration of *Cryptosporidium parvum* in sandy soils and aquifer sediments, *Environ. Sci. Technol.*, 34, 62–70.
- Harvey, R. W., L. H. George, R. L. Smith, and D. R. LeBlane (1989), Transport of microspheres and indigenous bacteria through a sandy aquifer: Results of natural and forced-gradient tracer experiments, *Environ. Sci. Technol.*, 23, 51–56.
- Harvey, R. W., N. E. Kinner, A. Bunn, D. Macdonald, and D. Metge (1995), Transport behavior of groundwater protozoa and protozoan-sized microspheres in sandy aquifer sediments, *Appl. Environ. Microbiol.*, 61, 209–217.
- Hejkal, T. W., B. Keswick, R. L. Labelle, C. P. Gerba, Y. Sanchez, G. Dreesman, B. Hafkin, and J. L. Melnick (1982), Viruses in a community water-supply associated with an outbreak of gastroenteritis and infectious-hepatitis, *J. Am. Water Works Assoc.*, 74, 318–321.
- Hornberger, G. M., A. L. Mills, and J. S. Herman (1992), Bacterial transport in porous media: Evaluation of a model using laboratory observations, *Water Resour. Res.*, 28, 915–938.
- Hu, S. W., X. Q. Ren, M. Bachman, C. E. Sims, G. P. Li, and N. Allbritton (2002), Surface modification of poly(dimethylsiloxane) microfluidic devices by ultraviolet polymer grafting, *Anal. Chem.*, 74, 4117–4123.
- Huettel, M., and A. Rusch (2000), Transport and degradation of phytoplankton in permeable sediment, *Limnol. Oceanogr.*, 45, 534–549.
- James, S. C., and C. V. Chrysikopoulos (2003), Effective velocity and effective dispersion coefficient for finite-sized particles flowing in a uniform fracture, *J. Colloid Interface Sci.*, 263, 288–295.
- Johnson, P. R., N. Sun, and M. Elimelech (1996), Colloid transport in geochemically heterogeneous porous media: Modeling and measurements, *Environ. Sci. Technol.*, 30, 3284–3293.
- Lanning, L. M., and R. M. Ford (2002), Glass micromodel study of bacterial dispersion in spatially periodic porous networks, *Biotechnol. Bioeng.*, 78, 556–566.
- Mailloux, B. J., T. C. Onstott, G. Moline, H. Dong, M. DeFlaun, M. Fuller, K. Gillespie, and S. Streger (1999), The determination of aqueous concentration profiles within intact sediment cores during transport experiments, paper presented at the Fourth International Symposium on Subsurface Microbiology, Int. Soc. of Subsurface Microbiol., Vail, Colo., 22–27 Aug.
- McDowell-Boyer, L. M., J. R. Hunt, and N. Sitar (1986), Particle transport through porous media, *Water Resour. Res.*, 22, 1901–1921.
- McGechan, M. B., N. J. Jarvis, P. S. Hooda, and A. J. A. Vinten (2002), Parameterization of the MACRO model to represent leaching of colloidal attached inorganic phosphorus following slurry spreading, *Soil Use Manage.*, 18, 61–67.
- Morley, L. M., G. M. Hornberger, A. L. Mills, and J. S. Herman (1998), Effects of transverse mixing on transport of bacteria through heterogeneous porous media, *Water Resour. Res.*, 34, 1901–1908.
- Nagasaki, S., S. Tanaka, and A. Suzuki (1993), Fast transport of colloidal particles through quartz-packed columns, *J. Nucl. Sci. Technol.*, 30, 1136–1144.
- Palmer, A., T. G. Mason, J. Y. Xu, S. C. Kuo, and D. Wirtz (1999), Diffusing wave spectroscopy microrheology of actin filament networks, *Biophys. J.*, 76, 1063–1071.
- Pang, L. P., M. Close, and M. Noonan (1998), *Rhodamine WT* and *Bacillus subtilis* transport through an alluvial gravel aquifer, *Ground Water*, 36, 112–122.
- Pieper, A. P., J. N. Ryan, R. W. Harvey, G. L. Amy, T. H. Illangasekare, and D. W. Metge (1997), Transport and recovery of bacteriophage PRD1 in a

- sand and gravel aquifer: Effect of sewage-derived organic matter, *Environ. Sci. Technol.*, *31*, 1163–1170.
- Quake, S. R., and A. Scherer (2000), From micro- to nanofabrication with soft materials, *Science*, *290*, 1536–1540.
- Russo, D. (2002), A note on the effective parameters of the convection-dispersion equation, *Water Resour. Res.*, *38*(2), 1017, doi:10.1029/2000WR000068.
- Sahimi, M., B. D. Hughes, L. E. Scriven, and H. T. Davis (1986), Dispersion in flow through porous-media, 1. One-phase flow, *Chem. Eng. Sci.*, *41*, 2103–2122.
- Scheibe, T. D., and B. D. Wood (2003), A particle-based model of size or anion exclusion with application to microbial transport in porous media, *Water Resour. Res.*, *39*(4), 1080, doi:10.1029/2001WR001223.
- Shonnard, D. R., R. T. Taylor, M. L. Hanna, C. O. Boro, and A. G. Duba (1994), Injection-attachment of methylosinus-trichosporium OB3b in a two-dimensional miniature sand-filled aquifer simulator, *Water Resour. Res.*, *30*, 25–35.
- Sinclair, J. L., and W. C. Ghiorse (1987), Distribution of protozoa in subsurface sediments of a pristine groundwater study site in Oklahoma, *Appl. Environ. Microbiol.*, *53*, 1157–1163.
- Sinton, L. W., M. J. Noonan, R. K. Finlay, L. Pang, and M. E. Close (2000), Transport and attenuation of bacteria and bacteriophages in an alluvial gravel aquifer, *N. Z. J. Mar. Freshwater*, *34*, 175–186.
- Sirivithayapakorn, S., and A. Keller (2003), Transport of colloids in saturated porous media: A pore-scale observation of the size exclusion effect and colloid acceleration, *Water Resour. Res.*, *39*(4), 1109, doi:10.1029/2002WR001583.
- Small, H. (1974), Hydrodynamic chromatography—Technique for size analysis of colloidal particles, *J. Colloid Interface Sci.*, *48*, 147–161.
- Straube, W. L., C. C. Nestler, L. D. Hansen, D. Ringleberg, P. H. Pritchard, and J. Jones-Meehan (2003), Remediation of polyaromatic hydrocarbons (PAHs) through landfarming with biostimulation and bioaugmentation, *Acta Biotechnol.*, *23*, 179–196.
- Woessner, W. W., P. N. Ball, D. C. DeBorde, and T. L. Troy (2001), Viral transport in a sand and gravel aquifer under field pumping conditions, *Ground Water*, *39*, 886–894.
- Zhang, P., W. P. Johnson, M. J. Piana, C. C. Fuller, and D. L. Naftz (2001), Potential artifacts in interpretation of differential breakthrough of colloids and dissolved tracers in the context of transport in a zero-valent iron permeable reactive barrier, *Ground Water*, *39*, 831–840.
- Zheng, C., and G. D. Bennett (1995), *Applied Contaminant Transport Modeling: Theory and Practice*, 440 pp., Van Nostrand Reinhold, Hoboken, N. J.

M. Auset and A. A. Keller, Bren School of Environmental Science and Management, 2324 Bren Hall, University of California, Santa Barbara, Santa Barbara, CA 93106, USA. (mauset@bren.ucsb.edu)

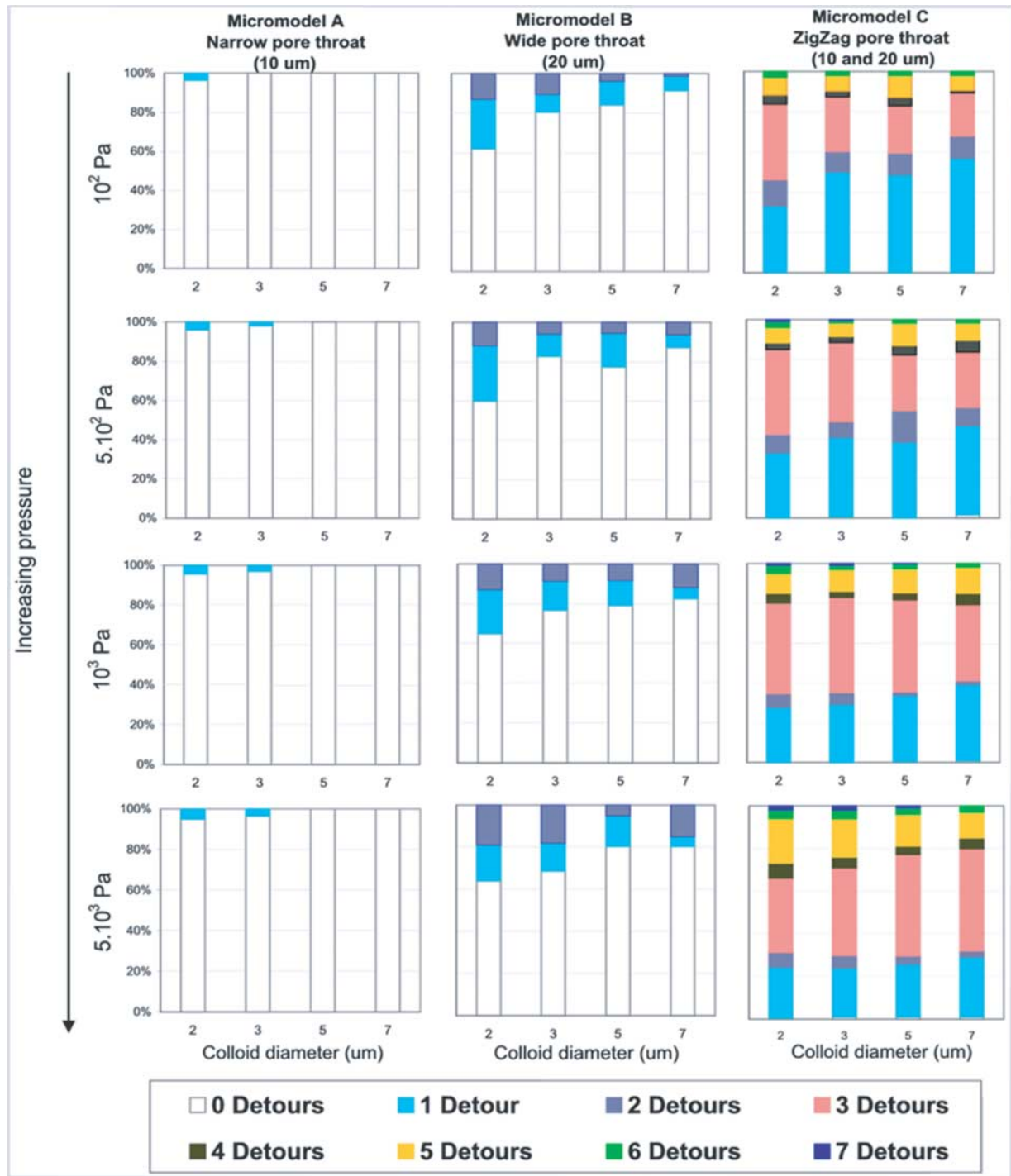


Figure 5. Frequency and number of detours in the regular narrow micromodel (first column), in the regular wide (second column), and in the zigzag micromodel for four colloid sizes and four pressures (third column).

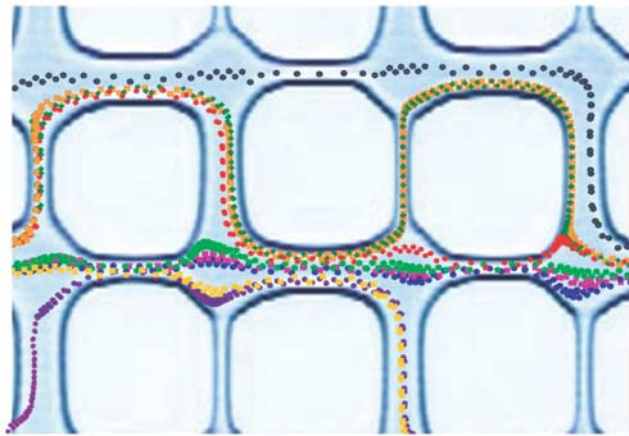


Figure 6. Detail of 2 μm colloid trajectories in the zigzag micromodel analyzed using IDL[®]. The colors indicate different particles tracked at different times but superimposed here to illustrate the different pathways.